Rozelle LT, Cadotte JE, Corneliussen RD and Erickson EE (1967) *Development of New Reverse Osmosis Membranes for Desalination*, Report No. PB-206329. Springfield, IL: VA National Technical Information Service.
Rozelle LT, Cadotte JE, Cobian KE and Kopp CV Jr (1977) In: Souriragan S (ed.) *Nonpolysaccharide Membranes for Reverse Osmosis. NS-100 Membranes for Reverse Osmosis and Synthetic Membranes*, p. 249. Ottawa, Canada: National Research Council Canada.
Souriragan S (1970) *Reverse Osmosis*. New York: Academic Press.

# Phase Inversion Membranes

**M. Mulder**, University of Twente, Enschede, The Netherlands



## Introduction

Phase inversion is the most versatile technique with which to prepare polymeric membranes. A variety of morphologies can be obtained that are suitable for different applications, from microfiltration membranes with very porous structures, to more dense reverse osmosis membranes, to gas separation and pervaporation membranes, with a complete defect-free structure. **Table 1** gives an overview of the techniques that are commonly applied for the preparation of synthetic polymeric membranes.

Most commercially available membranes are prepared by phase inversion. This is a process by which a polymer is transformed from a liquid or soluble state to a solid state. The concept of phase inversion covers a range of different techniques such as immersion precipitation or 'diffusion-induced phase separation', thermal-induced phase separation, 'vapour-phase' precipitation and precipitation by controlled evaporation. The technique of phase inversion has been known for quite some time; the first paper on the preparation of porous nitrocellulose membranes by phase inversion appeared in 1907.

**Table 1** Frequently used techniques for the preparation of synthetic polymeric membranes

| *Process* | *Techniques* |
|---|---|
| Microfiltration | Phase inversion, stretching, track-etching |
| Ultrafiltration | Phase inversion |
| Nanofiltration | Phase inversion, interfacial polymerization [a] |
| Reverse osmosis | Phase inversion, interfacial polymerization [a] |
| Pervaporation | Dipcoating [a], plasma polymerization [a] |
| Gas separation | Phase inversion, dipcoating [a], plasma polymerization [a] |
| Vapour permeation | Dipcoating [a] |

[a]Support layer prepared by phase inversion.

After World War I the number of publications on membrane preparation and characterization increased significantly and led to the development of the first methods for producing porous nitrocellulose membranes in a reproducible way. The 'Membranfiltergesellschaft Sartorius-Werke' in Göttingen was the first company to produce microfiltration membranes on a commercial scale, based on the work of Zsigmondy. This early work on preparation and characterization was reviewed by Ferry in 1936.

Until World War II most membrane research was performed in Germany, but after the war the technology was transferred to USA. In 1960 Goetz developed a new method for the production of porous membranes. Some years later the Millipore Corporation was founded, which commercialized this production method. The membranes were typically microfiltration membranes and were still based on cellulosic materials. It was more than two decades before ultrafiltration membranes were developed. Alan Michaels, founder of the Amicon Corporation, promoted the development of ultrafiltration membranes. Until that time the research was still focused on cellulosics as material but it became clear that due to the limited thermal and chemical stability other materials were required. This resulted in the development of various ultrafiltration membranes from polyacrylonitrile, polysulfone and polyvinylidene fluoride. Today polymeric materials are still the most commonly employed materials both in ultrafiltration and microfiltration. The early companies such as Sartorius and Schleicher and Schuell still exist and have expanded their membrane business to the technical market. Recently the market for the production of drinking water and industrial water from surface water has become important. Here both microfiltration/ultrafiltration and nanofiltration/reverse osmosis are either used as a single separation unit or in combination with each other or with another technique. The nanofiltration and reverse osmosis membranes are either thin film composites or, less commonly, asymmetric phase inversion membranes. In the case of composite membranes a phase inversion mem-

brane is usually used as support (see Table 1). For gas separation, vapour permeation and pervaporation composite membranes are generally applied with a porous support membrane prepared by phase inversion. Some gas separation membranes, such as polyphenylene oxide, are prepared by immersion precipitation, which results in completely defect-free asymmetric membrane.

## Phase Inversion Membranes

Phase inversion is a process whereby a polymer is transformed in a controlled way from a solution state to a solid state. The concept of phase inversion covers a range of different techniques such as precipitation by controlled evaporation, thermal precipitation from the vapour phase and immersion precipitation. The majority of phase inversion membranes are prepared by immersion precipitation.

### Precipitation from the Vapour Phase

This method was used as early as 1918 by Zsigmondy. A cast film, consisting of a polymer and a solvent, is placed in a vapour atmosphere where the vapour phase consists of a nonsolvent saturated with the solvent. The high solvent concentration in the vapour phase prevents the evaporation of solvent from the cast film. Membrane formation occurs because of the penetration (diffusion) of nonsolvent into the cast film. This results in a porous membrane without a top layer. With immersion precipitation an evaporation step in air is sometimes introduced and, if the solvent is miscible with water, precipitation from the vapour will start at this stage. An evaporation stage is often introduced in the case of hollow fibre preparation by immersion precipitation ('wet–dry spinning') exchange between the solvent and nonsolvent from the vapour phase, leading to precipitation.

### Precipitation by Controlled Evaporation

In this method the polymer is dissolved in a mixture of solvent and nonsolvent where the solvent is more volatile than the nonsolvent. The composition shifts during evaporation to a higher nonsolvent and polymer content. This eventually leads to polymer precipitation, resulting in the formation of a skinned membrane.

### Thermally Induced Phase Separation

A solution of polymer in a mixed or single solvent is cooled to enable phase separation to occur. Evaporation of the solvent often allows the formation of a skinned membrane. This method is frequently used to prepare microfiltration membranes, as will be discussed later.

### Immersion Precipitation

Most commercially available membranes are prepared by immersion precipitation: a polymer solution (polymer plus solvent) is cast on a suitable support and immersed in a coagulation bath containing a nonsolvent. Precipitation occurs because of the exchange of solvent and nonsolvent. The membrane structure ultimately obtained results from a combination of mass transfer and phase separation.

All phase inversion processes are based on the same thermodynamic principles, as will be described in the next section.

## Phase Separation

The change in Gibbs free enthalpy of mixing ($dG$) for a two-component system $i$ and $j$, where the numbers of moles are $n_i$ and $n_j$, respectively, is given by:

$$dG = V\,dP - S\,dT + \left(\frac{dG}{dn_i}\right)_{T,P,n_i} dn_i + \left(\frac{dG}{dn_j}\right)_{T,P,n_i} dn_j \quad [1]$$

Here $V$ is the volume, $S$ the entropy, $P$ the pressure and $T$ the temperature ($K$). The chemical potential of a component $i$, which is the partial molar free enthalpy, is defined as:

$$\mu_i = \left(\frac{\partial G}{\partial n_i}\right)_{P,T,n_j,n_k,\ldots} \quad [2]$$

where $\mu_i$ is equal to the change in free enthalpy of a system containing $n_i$ moles when the pressure, temperature and the number of moles of all the other components are held constant. For a multicomponent system eqn [1] becomes:

$$dG = V\,dP - S\,dT + \sum \mu_i\,dn_i \quad [3]$$

The chemical potential $\mu_i$ is defined at temperature $T$, pressure $P$, and composition $x_i$. For the pure component ($x_i = 1$), the chemical potential may be written as $\mu_i^o$.

The free enthalpy $G_m$ of a mixture consisting of two components is given by the sum of the chemical potentials (the partial free enthalpy). If $G_m$ is expressed per mole, then:

$$G_m = x_1\mu_1 + x_2\mu_2 \quad [4]$$

The dependence of the free enthalpy on the composition of the mixture is shown schematically in **Figure 1**. The value of the $G_m$ at the $y$-axis represent

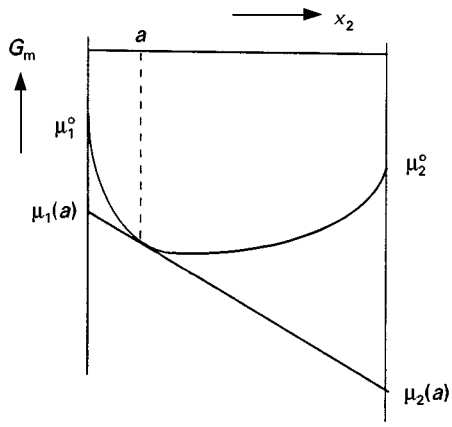


**Figure 1** Schematic drawing of the free enthalpy of a mixture at temperature $T$ as a function of the composition.

the chemical potential of the pure components. $\mu_1^o$ and $\mu_2^o$, respectively.

For ideal solutions the free enthalpy of mixing per mole is given by:

$$\Delta G_m = RT(x_1 \ln x_1 + x_2 \ln x_2) \qquad [5]$$

The solubility behaviour of polymer solutions differs completely from that of a solution containing components of low relative molecular mass because the entropy of mixing of the long polymeric chains is much lower. Flory and Huggins used a lattice model to describe the entropy of mixing of polymer solutions. In general for a binary system $\Delta G_m$ is given by:

$$\Delta G_m = RT(n_1 \ln \phi_1 + n_2 \ln \phi_2 + n_1\phi_2\chi) \qquad [6]$$

where an additional term has been added that was originally derived as an enthalpic contribution and which contains the Flory–Huggins interaction parameter $\chi$. In the original Flory theory $\chi$ was considered to be constant but for many systems it has been proven that this is not the case. In addition, $\chi$ is considered to be an excess free energy parameter containing all nonideality (including excess entropy). Differentiation of eqn [6] with respect to $n_1$ and $n_2$, respectively, gives the partial molar free enthalpy difference of component 1 ($\Delta\mu_1$) and ($\Delta\mu_2$) upon mixing:

$$\Delta\mu_1 = \mu_1 - \mu_1^o = \left(\frac{\partial \Delta G_m}{\partial n_1}\right)_{P,T,n_2}$$

$$= RT\left(\ln \phi_1 - \left(1 - \frac{V_1}{V_2}\right)\phi_2 + \chi\phi_2^2\right) \qquad [7]$$

and:

$$\Delta\mu_2 = \mu_2 - \mu_2^o = \left(\frac{\partial \Delta G_m}{\partial n_2}\right)_{P,T,n_1}$$

$$= RT\left(\ln \phi_2 - \left(1 - \frac{V_2}{V_1}\right)\phi_1 + \chi\frac{V_2}{V_1}\phi_1^2\right) \qquad [8]$$

In the case of polymer solutions the entropy term is very small and a positive enthalpy of mixing will cause demixing. Decreasing the temperature often causes an increase in the enthalpy of mixing.

**Figure 2** shows two plots of $\Delta G_m$ versus $\phi$ for two different temperatures. At temperature $T_1$ (Figure 2A), the system is completely miscible over the whole composition range. This is indicated by the tangent to the $\Delta G_m$ curve, which can be drawn at any composition. For example, at composition $a$ the intercept at $\phi_2 = 0$ gives $\mu_1(a)$ (the chemical potential of component 1 in the mixture of composition $a$) and the intercept at $\phi_2 = 1$ gives $\mu_2(a)$. This means that the chemical potentials of both components 1 and 2 de-

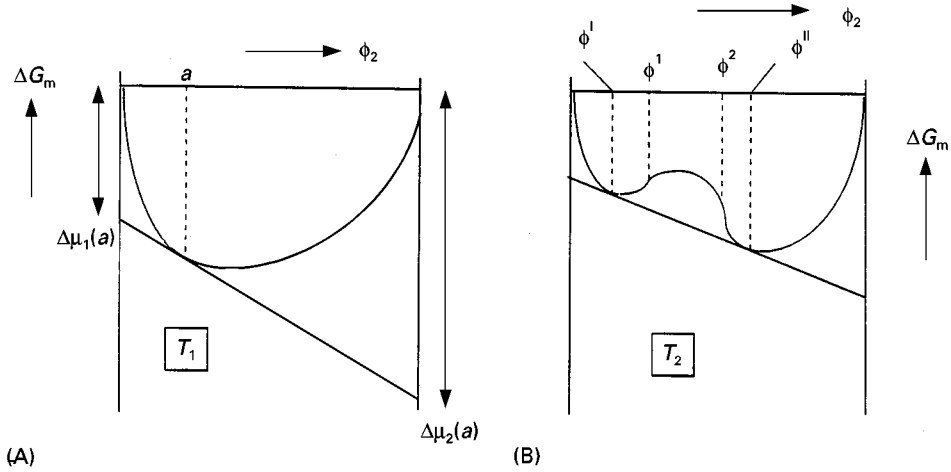


**Figure 2** Free energy of mixing as a function of composition for a binary mixture. $T_2 < T_1$ ($H_m > 0$).

crease (or $\Delta\mu_i < 0$). At temperature $T_2$ (Figure 2B), the curve of $\Delta G_m$ exhibits an upward bend between $\phi^I$ and $\phi^{II}$. These two points lie on the same tangent and are thus in equilibrium with each other. All the points on the tangent have the same derivative ($= \partial\Delta G_m/\partial n_i = \Delta\mu_i$), i.e. the chemical potentials are the same. In general, increasing the temperature leads to an increase in miscibility, which means that the enthalpy term becomes smaller. The two points on the tangent will approach each other and eventually they will coincide at the so-called critical point. This critical point is characterized by $(\partial^2\Delta G_m/\partial\phi_i^2) = 0$ and $(\partial^3\Delta G_m/\partial\phi_i^3) = 0$. Two points of inflection are also observed in Figure 2B, i.e. $\phi^1$ and $\phi^2$. A point of inflection is the point at which a curve changes from being concave to convex, or vice versa. These points are characterized by $(\partial^2\Delta G_m/\partial\phi_i^2 = 0)$. Plotting the locus of the minima in a $\Delta G_m$ versus $\phi$ diagram leads to the binodal curve. The locus of the inflection points is called the spinodal. A typical temperature–composition diagram is depicted in **Figure 3**.

The location of the miscibility gap for a given binary polymer–solvent system depends principally on the chain length of the polymer (see **Figure 4**). As the chain length increases the miscibility gap shifts towards the solvent axis as well as to higher temperatures. The critical point shifts towards the solvent axis, while the asymmetry of the binodal curve increases. The interaction between polymer and solvent is another important parameter, and this is expressed by the Flory–Huggins interaction parameter.

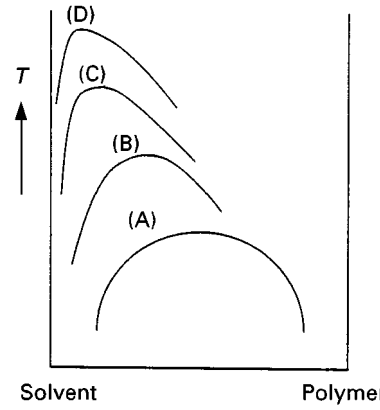


**Figure 4** Schematic drawing of a binary mixture with a region of immiscibility. Binodal (A): mixture of two components of low relative molecular mass; binodals (B), (C), (D): mixtures of a solvent with low relative molecular mass and a polymer with increasing relative molecular mass.

The location of the phase diagram in a binary or ternary system can be determined experimentally, e.g. by cloud point measurements, or theoretically by applying Flory–Huggins thermodynamics with suitable values for the interaction parameters.

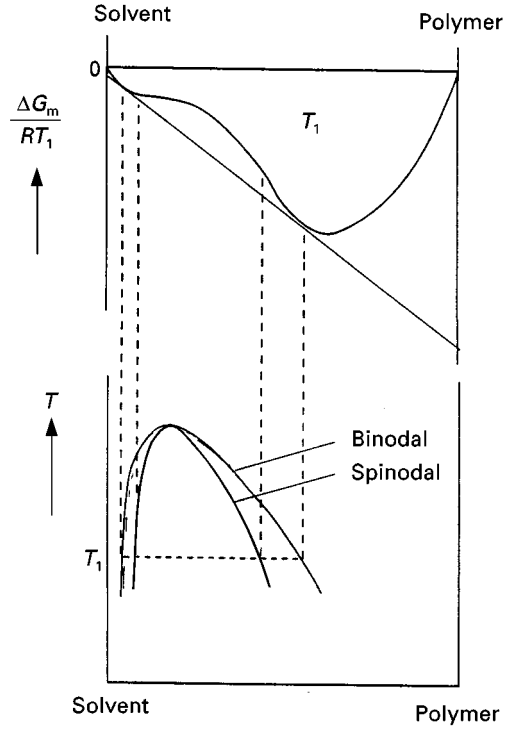


**Figure 3** Temperature–composition phase diagram for a binary polymer–solvent system.

## Demixing Processes

### Liquid–Liquid Demixing (Binary Systems)

To understand the mechanism of liquid–liquid demixing more easily, a binary system consisting of a polymer and a solvent will be considered. The starting point for preparing phase inversion membranes is a thermodynamically stable solution (see **Figure 5**), for example one with the composition $A$ at a temperature $T_1$ (with $T_1 > T_c$). All compositions with a temperature $T > T_c$ are thermodynamically stable. As the temperature decreases demixing of the solution will occur when the binodal is reached. The solution demixes into two liquid phases and this is referred to as liquid–liquid demixing.

Suppose that the temperature is decreased from $T_1$ to $T_2$. The composition $A$ at temperature $T_2$ lies inside the demixing gap and is not stable thermodynamically. The curve of $\Delta G_m$ at temperature $T_2$ is also given in Figure 5. At temperature $T_2$ all compositions between $\phi^I$ and $\phi^{II}$ can reduce their free enthalpies of mixing by demixing into two phases with compositions $\phi^I$ and $\phi^{II}$, respectively (see Figure 3). These two phases are in equilibrium with each other since they lie on the same tangent to the $\Delta G_m$ curve, i.e. the

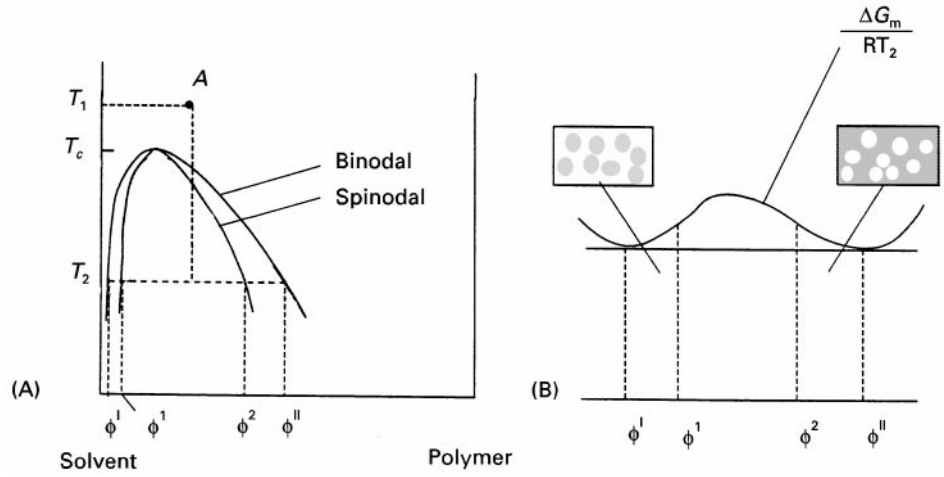


**Figure 5** Demixing of a binary polymer solution by deceasing the temperature. $T_C$ is the critical temperature.

chemical potential in phase $\phi^I$ must be equal to that of phase $\phi^{II}$.

**Figure 6** gives the curve of $\Delta G_m$ plotted against composition at a given temperature (e.g. $T_2$), together with the first and second derivative. Two regions can clearly be observed from the second derivative (the lowest figure). Over the interval $\phi^1 < \phi < \phi^2$ the second derivative of $\Delta G_m$ with respect to $\phi$ is negative, implying that the solution is thermodynamically unstable and will demix spontaneously into very small interconnected regions of composition $\phi^I$ and $\phi^{II}$:

$$\frac{\partial^2 \Delta G_m}{\partial \phi^2} < 0 \qquad (\phi^1 < \phi < \phi^2) \qquad [9]$$

The amplitude of small fluctuations in the local concentration increases in time, as shown schematically in **Figure 7**. In this way a lacy structured membrane is obtained, and the type of demixing observed is called spinodal demixing. Over the intervals $\phi^I < \phi < \phi^1$ and $\phi^2 < \phi < \phi^{II}$, the second derivative of $\Delta G_m$ with respect to $\phi$ is positive and the solution is metastable. This means that there is no driving force for spontaneous demixing and the solution is stable towards small fluctuations in composition. Demixing

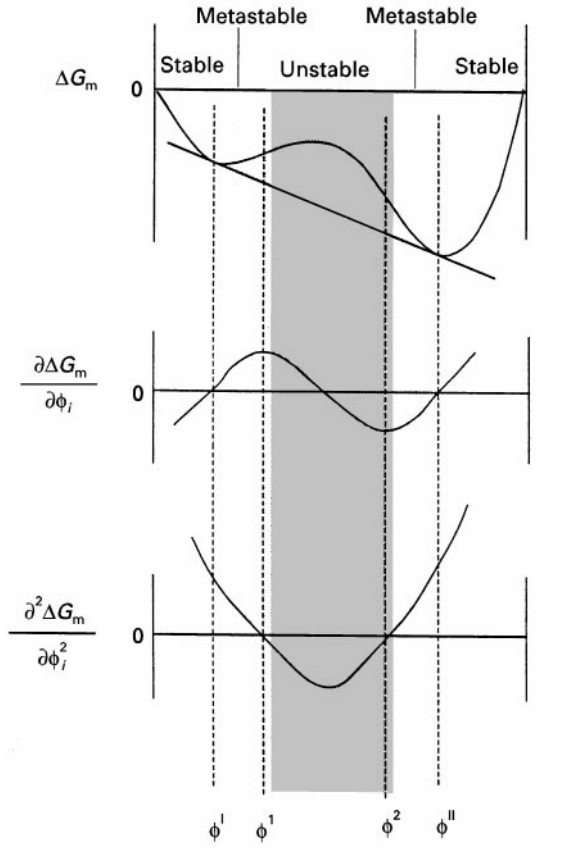


**Figure 6** Plots of $\Delta G_m$, the first derivative of $\Delta G_m$ and the second derivative of $\Delta G_m$ against $\phi$.

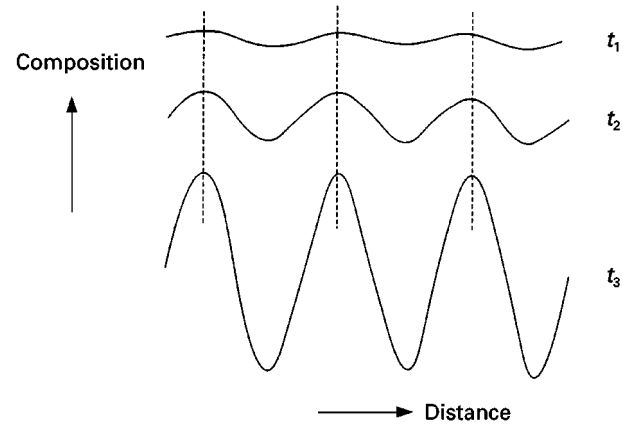


**Figure 7** Spinodal demixing: increase in amplitude with increasing time ($t_3 > t_2 > t_1$).

can commence only when a stable nucleus has been formed. A nucleus is stable when it lowers the free enthalpy of the system; hence over the interval $\phi^{I} < \phi < \phi^{1}$ the nucleus must have a composition near $\phi^{II}$, and over the interval $\phi^{2} < \phi < \phi^{II}$ it must have a composition near $\phi^{I}$:

$$\frac{\partial^2 \Delta G_m}{\partial \phi^2} > 0 \quad (\phi^{I} < \phi < \phi^{1}) \quad \text{and} \quad (\phi^{2} < \phi < \phi^{II}) \qquad [10]$$

After nucleation, these nuclei grow further in size by downhill diffusion whereas the composition of the continuous phase moves gradually towards that of the other equilibrium phase. The type of structure obtained after liquid–liquid demixing by nucleation and growth depends on the initial concentration.

Starting with a very dilute polymer solution (see Figure 5), the critical point will be passed on the left-hand side of the diagram and liquid–liquid demixing will start when the binodal curve is reached and a nucleus is formed with a composition near $\phi^{II}$. The nucleus formed will grow further until thermodynamic equilibrium is reached (nucleation and growth of the polymer-rich phase). A two-phase system is formed consisting of concentrated polymer droplets of composition $\phi^{II}$ dispersed in a dilute polymer solution with composition $\phi^{I}$. In this way a latex type of structure is obtained, which has little mechanical strength. When the starting point is a more concentrated solution (composition *A* in Figure 5), demixing will occur by nucleation and growth of the polymer-lean phase (composition $\phi^{I}$). Droplets with a very low polymer concentration will now continue to grow until equilibrium has been reached.

As can be seen from Figure 5, the location of the critical point is close to the solvent axis. Hence the binodal curve for a polymer–solvent system will be reached on the right-hand side of the critical point, indicating that liquid–liquid demixing will occur by nucleation of the polymer-lean phase. These tiny droplets will grow further until the polymer-rich phase solidifies. If these droplets have the opportunity to coalesce before the polymer-rich phase has solidified, an open porous system will result.

### Liquid–Liquid Demixing (Ternary Systems)

In addition to temperature changes, changes in composition brought about by the addition of a third component, a nonsolvent, can also cause demixing. Under these circumstances we have a ternary system consisting of a solvent, a nonsolvent and a polymer. The liquid–liquid demixing area must now be represented as a three-dimensional surface. The free enthalpy of mixing is a function of the composition, as can be seen from **Figure 8**, where the $\Delta G_m$ surface is depicted at a certain temperature. All pairs of compositions with a common tangent plane to the $\Delta G_m$ surface constitute the solid line projected in the phase diagram, the binodal. **Figure 9** shows a schematic illustration of the temperature dependency of such a three-dimensional liquid–liquid demixing surface for a ternary system. The demixing area takes the form of a part of a beehive. As the temperature increases the demixing area decreases, and if the temperature is sufficiently high the components are miscible in all proportions. From this figure an isothermal cross-section can be obtained at any temperature as shown in **Figure 10**.

The corners of the triangle in Figure 10 represent the pure components polymer, solvent and

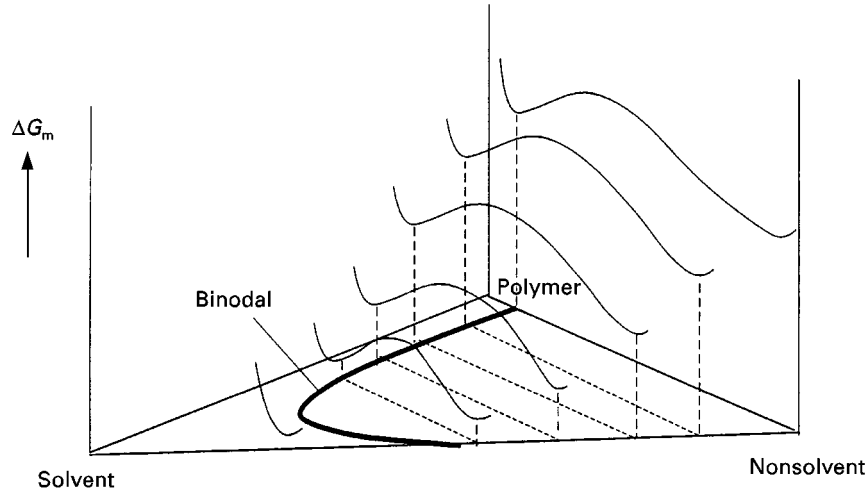


**Figure 8** Schematic drawing of the free enthalpy of mixing ($\Delta G_m$) as a function of the composition for a ternary system consisting of polymer, solvent and nonsolvent.

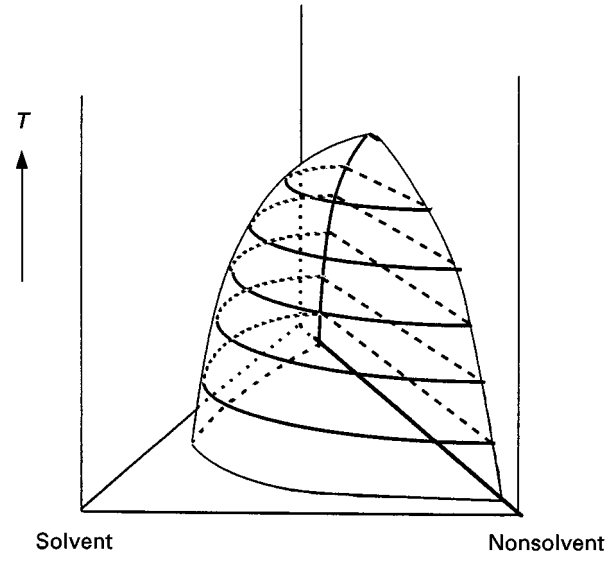


**Figure 9** Three-dimensional representation of the binodal surface at various temperatures for a ternary system consisting of polymer, solvent and a nonsolvent.

nonsolvent. A point located on one of the sides of the triangle represents a mixture consisting of the two corner components. Any point within the triangle represents a mixture of the three components. In this region a spinodal curve and binodal curve can be observed. The tie lines connect points on the binodal curve that are in equilibrium. A composition within this two-phase region always lies on a tie line and splits into two phases represented by the two intersections between the tie line and the binodal curve. As in the binary system, one end point of the tie line is rich in polymer and the other end point is poor in polymer. The binodal curve may be calculated numerically. The tie lines connect the two coexisting phases that are in equilibrium with each other, and these have the same chemical potential. By minimizing the following function the compositions of the end points may be obtained:

$$F = \sum f_i^2 \qquad [11]$$

with $f_i = (\Delta\mu_i' - \Delta\mu_i'')$ and $i = 1, 2, 3$. The polymer-lean phase is indicated by a single prime ($'$) and the polymer-rich phase is indicated by a double prime ($''$).

The initial procedure for membrane formation from such ternary systems is always to prepare a homogeneous (thermodynamically stable) polymer solution. This will often correspond to a point on the polymer–solvent axis. However, it is also possible to add nonsolvent as long as all the components are still miscible. Demixing will occur by the addition of such an amount of nonsolvent that the solution becomes thermodynamically unstable.

When the binodal curve is reached liquid–liquid demixing will occur. As in the binary system, the side from which the critical point is approached is important. In general, the critical point is situated at low to very low polymer concentrations (see Figure 10). When the metastable miscibility gap is entered at compositions above the critical point, nucleation of the polymer-lean phase occurs. The tiny droplets formed consist of a mixture of solvent and nonsolvent with very little polymer dispersed in the polymer-rich phase, as described in the binary example (see Figure 5). These droplets can grow further until the surrounding continuous phase solidifies via crystallization, gelation or when the glass transition temperature has been passed (in the case of glassy polymers). Coalescence of the droplets before solidification leads to the formation of an open porous structure.

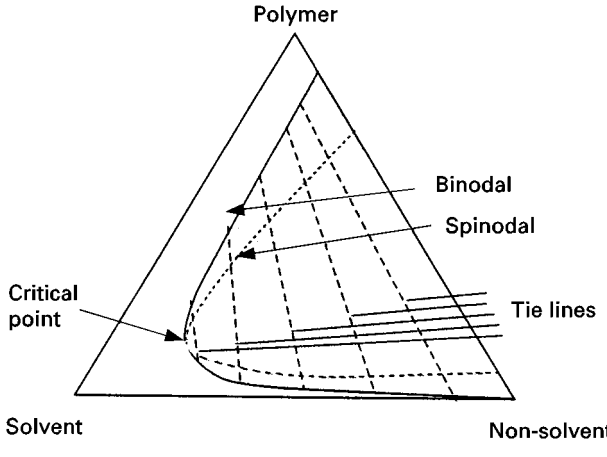


**Figure 10** Schematic representation of a ternary system with a liquid–liquid demixing gap.

### Solid–Liquid Demixing (Crystallization)

Many polymers are partially crystalline. They consist of an amorphous phase without any ordering and an ordered crystalline phase. Crystallization may occur if the temperature of the solution is below the melting point of the polymer. **Figure 11** shows the free enthalpy of mixing ($\Delta G_m$) for a binary system of polymer and solvent (or diluent) that shows no liquid–liquid demixing. However, below the melting point the chemical potential of the polymer in the solid state will be smaller than that in the solution. Therefore, the solution can lower its free enthalpy by phase separation into a pure crystalline solid state ($\phi_2$) and a liquid state ($\phi_a$ in Figure 11) that are in equilibrium with each other ($\Delta\mu_{2,L} = \Delta\mu_{2,S}$). The corresponding melting temperature for this mixture $\phi_a$ is $T_1$. This is shown schematically in Figure 11B. $T_m^o$ is the melting point of the pure polymer and the melting

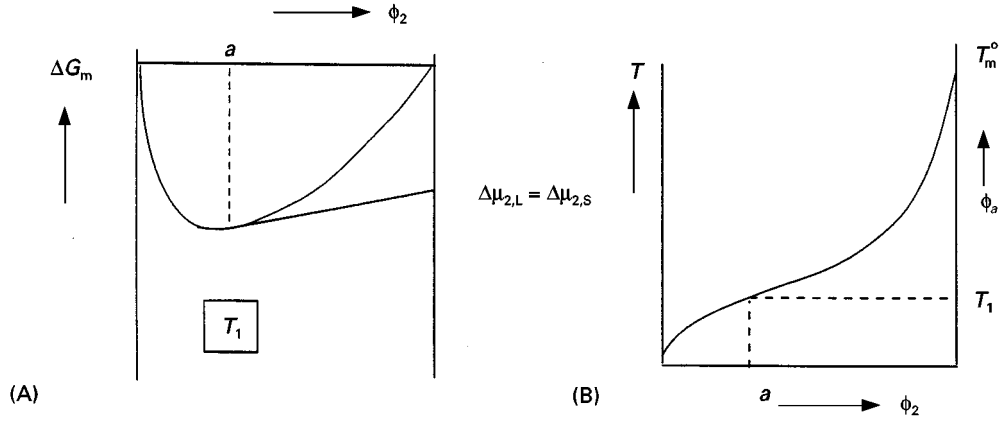


**Figure 11** Schematic drawing of the free enthalpy of mixing for a binary system in which component 2 is able to crystallize (A) and the melting point curve as a function of the composition (B). $\phi_a$ is the volume fraction at point *a*.

point depression for a binary polymer–solvent system, as derived by Flory, is given below:

$$\frac{1}{T_m} - \frac{1}{T_m^o} = \frac{R}{\Delta H_f}\frac{V_2}{V_1}(\phi_1 - \chi\phi_1^2) \qquad [12]$$

Here $\phi_1$ is the volume fraction of solvent and $\chi$ is the polymer–solvent interaction parameter; $T_m$ is the melting temperature of the diluted polymer; $\Delta H_f$ is the heat of fusion per mole of repeating units; and $V_1$ and $V_2$ are the molar volume of the solvent and of the polymer repeating unit, respectively.

For a ternary system with a semicrystalline polymer a similar ternary diagram can be constructed, as shown in **Figure 12**. However, it is somewhat more complex since solid–liquid demixing occurs in addition to liquid–liquid demixing. Except for the homogeneous region (I) where all components are miscible with each other and a region where liquid–liquid demixing occurs (II), other phases can be observed. The curve PQ is the crystallization curve and a composition somewhere in the region of P–Q–polymer will contain crystalline pure polymer that is in equilibrium with a composition somewhere on the crystallization line PQ. A possible morphology of a semicrystalline polymer is shown schematically in **Figure 13**. Spherulitic structures are frequently observed in semicrystalline polymers.

Many morphologies are possible ranging from a completely crystalline to a completely amorphous conformation. The formation of crystalline regions in a given polymer depends on the time allowed for crystallization from the solution. In very dilute solutions the polymer chains can form single crystals of the lamellar type, whereas in medium and concentrated solutions more complex morphologies occur, e.g. dendrites and spherulites.

Membrane formation is generally a fast process and only polymers that are capable of crystallizing rapidly (e.g. polyethylene, polypropylene, aliphatic polyamides) will exhibit an appreciable amount of

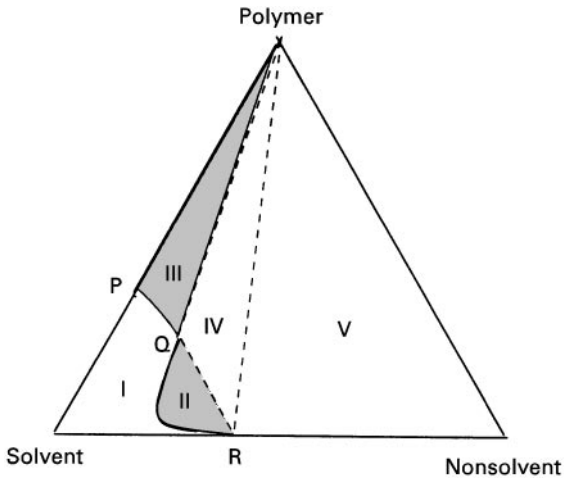


**Figure 12** Ternary system of a semicrystalline polymer, solvent and nonsolvent system. I, homogeneous, II, liquid–liquid; III, Solid–liquid; IV, solid–liquid–liquid; V, solid–liquid.

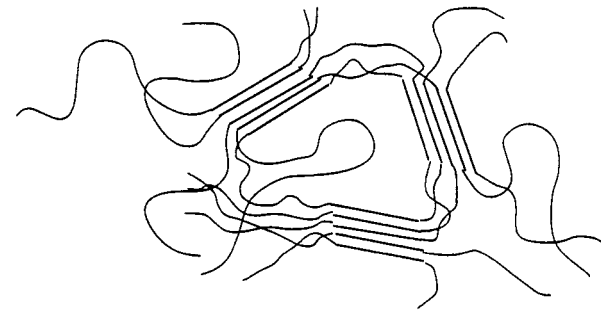

**Figure 13** Morphology of a semicrystalline polymer (fringed micelle structure).

crystallinity. Other semicrystalline polymers contain a low to very low crystalline content after membrane formation. For example, PPO (2,6-dimethylphenylene oxide) shows a broad melting endotherm at 245°C. Ultrafiltration membranes derived from this polymer, prepared by phase inversion, hardly contain any crystalline material, indicating that membrane formation was too rapid to allow crystallization.

### Gelation

Gelation is a phenomenon of considerable importance during membrane formation, especially for the formation of the top layer. It was mentioned in the previous section that a large number of semicrystalline polymers exhibit a low crystalline content in the final membrane because membrane formation is too fast. However, these polymers generally undergo another solidification process, i.e. gelation. Gelation can be defined as the formation of a three-dimensional network by chemical or physical cross-linking. Chemical cross-linking, the covalent bonding of polymer chains by means of a chemical reaction, will not be considered here.

When gelation occurs, a dilute or more viscous polymer solution is converted into a system of infinite viscosity, i.e. a gel. A gel may be considered as a highly elastic, rubber-like solid. A gelled solution does not demonstrate any flow when a tube containing the solution is tilted. Gelation is not a phase separation process, and it may also take place in a homogeneous system consisting of a polymer and a solvent. Many polymers used as membrane materials exhibit gelation behaviour, e.g. cellulose acetate, poly(phenylene oxide), polyacrylonitrile, poly(methyl) methacrylate, poly(vinyl chloride) and poly(vinyl alcohol). Physical gelation may occur by various mechanisms dependent on the type of polymer and solvent or solvent–nonsolvent mixture used. In the case of semicrystalline polymers especially, gelation is often initiated by the formation of microcrystallites. These microcrystallites, which are small ordered regions, are in fact the nuclei for the crystallization process but without the ability to grow further. However, if these microcrystallites can connect various polymeric chains together, a three-dimensional network will be formed. Because of their crystalline nature these gels are thermo-reversible, i.e. upon heating the crystallites melt and the solution can flow. Upon cooling, the solution again gels. The formation of helices often occurs during the gelation process. Gelation may also occur by other mechanisms, e.g. the addition of complexing ions ($Cr^{3+}$) or by hydrogen bonding.

Gelation is also possible in completely amorphous polymers (e.g. atactic polystyrene). In a number of systems the involvement of gelation in the membrane formation process often involves a sol–gel transition. This is shown schematically in **Figure 14**. As can be seen from this figure, a sol–gel transition occurs where the solution gels. The addition of a nonsolvent induces the formation of polymer–polymer bonds and gelation occurs at a lower polymer concentration. These sol–gel transitions have been observed in a number of systems, e.g. cellulose acetate/acetone/water, cellulose acetate/dioxane/water, poly(phenylene oxide)/trichloroethylene/octanol and poly(phenylene oxide)/trichloroethylene/methanol.

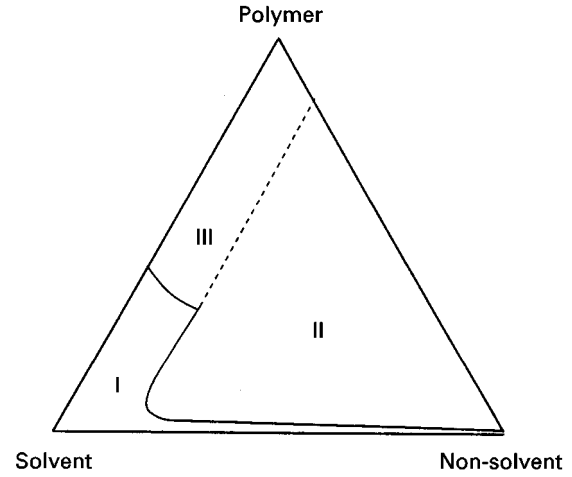


**Figure 14** Isothermal cross-section of a ternary system containing a one-phase region (I), a two-phase region (II) and a gel region (III).

### Vitrification

There are polymers that show neither crystallization nor gelation behaviour. Nevertheless, these polymers finally solidify during a phase inversion process. This solidification process may be defined as vitrification, which is the stage where the polymer chains are frozen in a glassy state, i.e. it is a phase where the glass transition temperature has been passed and the mobility of the polymer chains has been reduced drastically. In the absence of gelation or crystallization, vitrification is the mechanism of solidification in any membrane-forming system with an amorphous glassy polymer.

The glass transition of a polymer is reduced by the presence of an additive, i.e. a solvent or nonsolvent. This glass transition depression can been described by various theories, the Kelley–Bueche theory being widely used. A schematic phase diagram of the system PPO/trichloroethylene/methanol is shown in **Figure 15**. Four regions can be observed:

1. a one-phase region where all the components are miscible with each other;

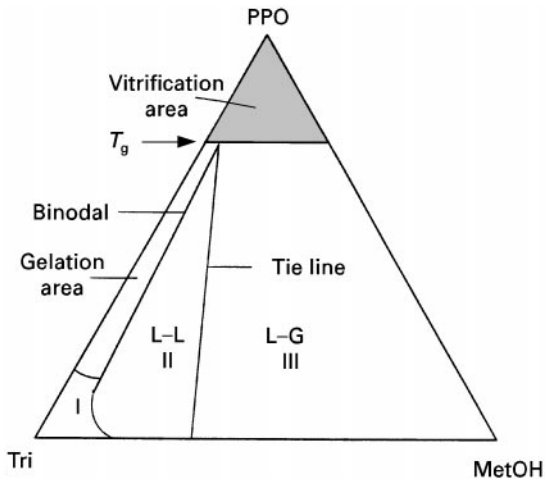


**Figure 15** Schematic phase diagram of the quasi ternary system PPO/trichloroethylene/methanol.

2. a gel region where the polymer is able to form a three-dimensional network, providing that certain conditions have been established (a sol–gel transition for the system PPO/DMAc has been determined, however a minimum time of 1 h is necessary for gel formation whereas in immersion precipitation the timescale is much shorter);
3. a glassy region or vitrification region where the glass transition or the polymer has been passed. During immersion precipitation the diffusion of solvent and nonsolvent proceeds according to their corresponding driving forces independent of whether gelation occurs. The final solidification may be a combined gelation/vitrification process, or in absence of gelation vitrification will be the dominant process.
4. a two-phase region where liquid–liquid demixing occurs. In the figure only one tie line is given in which the polymer-rich phase has entered the vitrification area. On the left side of this tie line (II) the (equilibrium) system is still a liquid, whereas on the right side (III) vitrification of the polymer-rich phase had occurred.

## Membrane Formation

### Thermally Induced Phase Separation (TIPS)

Before describing immersion precipitation in detail, a short description of thermal precipitation or 'thermally induced phase separation' (TIPS) is given.

This process allows the ready preparation of porous membranes from a binary system consisting of a polymer and a solvent. Generally, the solvent has a high boiling point, e.g. sulfolane (tetramethylene sulfone, bp 287°C) or oil (e.g. nujol). The starting point is a homogeneous solution, for example composition $A$ at temperature $T_1$ (see Figure 5).

This solution is cooled slowly to the temperature $T_2$. When the binodal curve is attained liquid–liquid demixing occurs and the solution separates into two phases, one rich in polymer and the other poor in polymer. When the temperature is decreased further to $T_2$, the composition of the two phases follow the binodal curve and eventually the compositions $\phi^{I}$ and $\phi^{II}$ are obtained. At a certain temperature the polymer-rich phase solidifies by crystallization (polyethylene), gelation (cellulose acetate) or on passing the glass transition temperature (atactic polymethylacrylate). Frequently, semicrystalline polymers are used (polyethylene, polypropylene, aliphatic polyamides) which crystallize relatively fast, and hence a solid–liquid phase transition should be included.

**Figure 16** shows how the liquid–liquid (L–L) demixing area and the solid–liquid (S–L) for a binary system. In the case of glassy amorphous polymers the melting line may be replaced by a vitrification line. This concept may be applied to various systems, **Table 2** provides some examples of this thermally induced phase separation (TIPS) process.

### Immersion Precipitation

An interesting question remains after all of these theoretical considerations: what factors are important in order to obtain the desired (asymmetric) morphology after immersion of a polymer–solvent mixture in a nonsolvent coagulation bath? Another interesting question is: why is a more open (porous) top layer obtained in some cases whereas in other cases a very dense (nonporous) top layer supported by an (open) sponge-like structure develops? To answer these questions and to promote an understanding of the basic principles leading to membrane formation

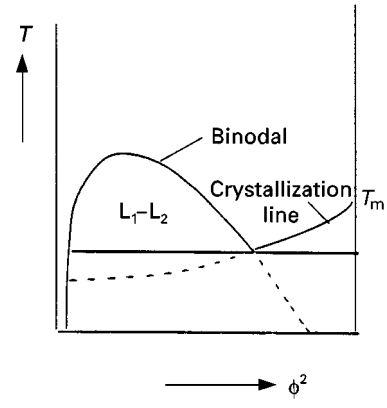


**Figure 16** Construction of a $T$–$\phi$ diagram for a binary system polymer–solvent. The solidification line is the glass transition temperature line.

**Table 2** Some examples of thermally-induced phase separation systems

| *Polymer* | *Solvent* |
|---|---|
| Polypropylene | Mineral oil (nujol) |
| Polyethylene | Mineral oil (nujol) |
| Polyethylene | Dihydroxy tallow amine |
| Poly(methyl) methacrylate | Sulfolane |
| Cellulose acetate/PEG | Sulfolane |
| Cellulose acetate/PEG | Dioctyl phthalate |
| Nylon-6 | Triethylene glycol |
| Nylon-12 | Triethylene glycol |
| Poly(4-methyl pentene) | Mineral oil (nujol) |

via immersion precipitation, a qualitative description will be given. For the sake of simplicity, the concept of membrane formation will be described in terms of three components: nonsolvent (1), solvent (2) and polymer (3). The effect of additives such as second polymer or material of low relative molecular mass will not be considered because the number of possibilities would then becomes so large and every (quarternary) or multicomponent system has its own complex thermodynamic and kinetic descriptions.

Immersion precipitation membranes in their most simple form are prepared in the following way. A polymer solution consisting of a polymer (3) and a solvent (2) is cast as a thin film upon a support (e.g. a glass plate) and then immersed in a nonsolvent (1) bath. The solvent diffuses into the coagulation bath ($J_2$) while the nonsolvent will diffuse into the cast film ($J_1$). After a given period of time the exchange of solvent and nonsolvent has proceeded so far that the solution becomes thermodynamically unstable and demixing takes place. Finally a solid polymeric film is obtained with an asymmetric structure. A schematic representation of the film–bath interface during immersion is shown in **Figure 17**.

The local composition at any point in the cast film depends on time. However, it is not possible to measure composition changes very accurately with time because the thickness of the film is only of the order of a few microns. Furthermore, membrane formation can sometimes occur instantaneously, i.e. all the compositional changes must be measured as a function of place and time within a very small time interval. Nevertheless, these composition changes can be calculated. Such calculations provide a good insight into the influence of various parameters upon membrane structure and performance.

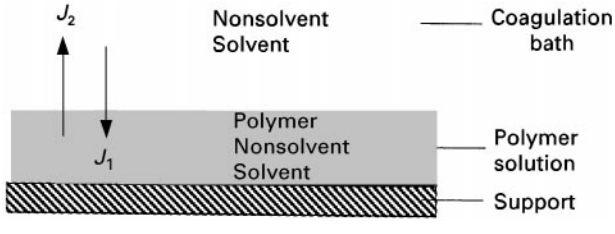


**Figure 17** Schematic representation of a film–bath interface. Components: nonsolvent (1), solvent (2) and polymer (3). $J_1$ is the nonsolvent flux and $J_2$ the solvent flux.

Different factors have a major effect upon membrane structure. These are:

- choice of polymer;
- choice of solvent and nonsolvent;
- composition of casting solution;
- composition of coagulation bath;
- gelation, vitrification and crystallization behaviour of the polymer;
- location of the liquid–liquid demixing gap;
- temperature of the casting solution and the coagulation bath; and
- evaporation time.

By varying one or more of these parameters, which are not independent of each other, the membrane structure can be changed from a very open porous form to a very dense nonporous variety.

Take polysulfone as an example. This is a polymer that is frequently used as a membrane material, both for microfiltration/ultrafiltration as well as a sublayer in composite membranes. These applications require an open porous structure, but in addition asymmetric membranes with a dense nonporous top layer can also be obtained that are useful for prevaporation or gas separation applications. Some examples are given in **Table 3** that clearly demonstrate the influence of various parameters on the membrane structure when the same system, DMAc/polysulfone (PSf), is employed in each case. To understand how it is possible to obtain such different structures with one and the same system, it is necessary to consider how each of the variables

**Table 3** Influence of preparation procedure on membrane structure

| |
|---|
| Evaporation PSf/DMAc ⇒ pervaporation/gas separation |
| Precipitation of 15% PSf/DMAc/THF in water ⇒ gas separation [a] |
| Precipitation of 35% PSf/DMAc in water ⇒ pervaporation/gas separation [b] |
| Precipitation of 15% PSf/DMAc in water ⇒ ultrafiltration |
| Precipitation of 15% PSf/DMAc in water/DMAc ⇒ microfiltration [c] |

[a] After an initial evaporation step.
[b] It will be shown later that integrally skinned asymmetric membranes can be prepared with completely defect-free top layers.
[c] To obtain an open (interconnected) porous membrane, an additive, e.g. poly(vinyl pyrrolidone) must be added to the polymer solution.

affects the phase inversion process. The ultimate structure arises through two mechanisms: (1) a diffusion processes involving solvent and nonsolvent occurring during membrane formation; and (2) demixing processes.

### Diffusional Aspects

Membrane formation by phase inversion techniques, e.g. immersion precipitation, is a nonequilibrium process that cannot be described by thermodynamics alone since kinetics have also to be considered. The composition of any point in the cast film is a function of place and time. To know what type of demixing process occurs and how it occurs, it is necessary to know the exact local composition at a given instant. However, this composition cannot be determined very accurately experimentally because the change in composition occurs extremely quickly (in often less than 1 s) and the film is very thin (less than 200 μm). However, it can be described theoretically. Cohen *et al*. were the first to describe mass transport in an immersion precipitation process. Since then many modified models have been published to describe better this highly nonideal complex multicomponent mass transfer system.

The change in composition may be considered to be determined by the diffusion of the solvent ($J_2$) and the nonsolvent ($J_1$) (see Figure 17) in a polymer fixed frame of reference. The fluxes $J_1$ and $J_2$ at any point in the cast film can be represented by a phenomenological relationship:

$$J_i = -\sum_{j=1}^{2} L_{ij}(\phi_i, \phi_j)\frac{\partial \mu_j}{\partial x} \qquad (i = 1, 2) \qquad [13]$$

where $-\partial\mu/\partial x$, the gradient in the chemical potential, is the driving force for mass transfer of component $i$ at any point in the film and $L_{ij}$ is the permeability coefficient. From eqn [13] the following relations may be obtained for the nonsolvent flux ($J_1$) and the solvent flux ($J_2$):

$$J_1 = -L_{11}\frac{\mathrm{d}\mu_1}{\mathrm{d}x} - L_{12}\frac{\mathrm{d}\mu_2}{\mathrm{d}x} \qquad [14]$$

$$J_2 = -L_{21}\frac{\mathrm{d}\mu_1}{\mathrm{d}x} - L_{22}\frac{\mathrm{d}\mu_2}{\mathrm{d}x} \qquad [15]$$

As can be seen from the above equations, the fluxes in a given polymer/solvent/nonsolvent system are determined by the gradient in the chemical potential as driving force, while they also appear in the phenomenological coefficients. This implies that a knowledge of the chemical potentials, or better the factors that determine the chemical potential, is of great importance. An expression for the free enthalpy of mixing has been given by Flory and Huggins. For a three-component system (polymer/solvent/nonsolvent), the Gibbs free energy of mixing ($\Delta G_\mathrm{m}$) is given by:

$$\Delta G_\mathrm{m} = RT(n_1 \ln \phi_1 + n_2 \ln \phi_2 + n_3 \ln \phi_3 + \chi_{12} n_1 \phi_2 + \chi_{13} n_1 \phi_3 + \chi_{23} n_2 \phi_3) \qquad [16]$$

where $R$ is the gas constant and $T$ is the absolute temperature. The subscripts refer to nonsolvent (1), solvent (2) and polymer (3). The number of moles and the volume fraction of component $i$ are $n_i$ and $\phi_i$, respectively. $\chi_{ij}$ is called the Flory–Huggins interaction parameter. In a ternary system there are three interaction parameters: $\chi_{13}$ (nonsolvent/polymer), $\chi_{23}$ (solvent/polymer) and $\chi_{12}$ (solvent/nonsolvent). $\chi_{12}$ can be obtained from data on excess free energy of mixing that have been compiled or from vapour–liquid equilibria. $\chi_{13}$ can be obtained from swelling measurements and $\chi_{23}$ can be obtained from vapour pressure or membrane osmometry. The interaction parameters account for the nonideality of the system and they contain an enthalpic as well as an entropic contribution. In the original Flory–Huggins theory they are assumed to be concentration independent, but several experiments have shown that these parameters generally depend on the composition. To account for such dependence the symbol $\chi$ is often replaced by another symbol, $g$, indicating concentration dependency.

From eqn [16] it is possible to derive the expressions for the chemical potentials of the components since:

$$\left(\frac{\partial \Delta G_\mathrm{m}}{\partial n_i}\right)_{P,T,n_i} = \Delta\mu_i = \mu_i - \mu_i^0 \qquad [17]$$

The eventual concentration dependency of the $\chi$ parameter must be taken into account in the differentiation procedure. The influence of the different interaction parameters $\chi$ (present in the driving forces) on the solvent flux and nonsolvent flux, and thus on the membrane structures obtained, will be described later.

The other terms present in the flux equations (eqns [16] and [17]) are phenomenological coefficients, and these must also be considered with respect to membrane formation. These coefficients are also mostly concentration dependent. There are two ways of expressing the phenomenological coefficients when the relationships for the chemical poten-

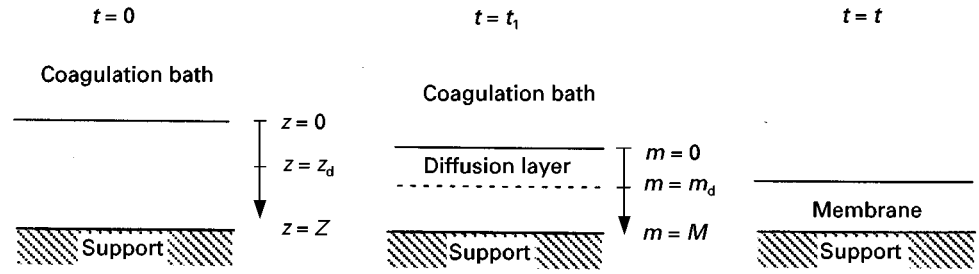


**Figure 18** Schematic drawing of the immersion process at different times.

tials are known: (1) in diffusion coefficients; and (2) in friction coefficients.

In most cases there is a (large) difference between the casting thickness and the ultimate membrane thickness. This implies that during the formation process the boundary between the nonsolvent bath and the casting solution moves, as is shown in **Figure 18**. For this reason, it is necessary to introduce a position coordinate to correct for this moving boundary.

The immersion process starts at time $t = 0$. At all times $t > 0$, solvent will diffuse out of the film and nonsolvent will diffuse in. If there is a net volume outflow (solvent flux larger than nonsolvent flux) then the film–bath interface is shifted from $z = 0$, i.e. the actual thickness is reduced. This process will continue until equilibrium is reached (at time $t = t$) and the membrane has been formed. In order to describe diffusion processes involving a moving boundary adequately, a position coordinate $m$ must be introduced (eqn [18]).

The film–bath interface is now always at position $m = 0$, independent of time. The position of the film–support interface is also independent of time (see Figure 18):

$$m(x, t) = \int_0^x \phi_3(x, t)\, \mathrm{d}x \qquad [18]$$

$$(\mathrm{d}m)_t = \phi_3\, (\mathrm{d}x)_t \qquad [19]$$

In the $m$-coordinate:

$$\frac{\partial(\phi_i/\phi_3)}{\partial t} = \frac{\partial J_i}{\partial m} \quad i = 1, 2 \qquad [20]$$

Combination of eqns [18]–[20] yields:

$$\frac{\partial(\phi_1/\phi_3)}{\partial t} = \frac{\partial}{\partial m}\left[\nu_1\phi_3 L_{11}\frac{\partial\mu_1}{\partial m}\right] + \frac{\partial}{\partial m}\left[\nu_1\phi_3 L_{12}\frac{\partial\mu_2}{\partial m}\right] \qquad [21]$$

$$\frac{\partial(\phi_2/\phi_3)}{\partial t} = \frac{\partial}{\partial m}\left[\nu_2\phi_3 L_{21}\frac{\partial\mu_1}{\partial m}\right] + \frac{\partial}{\partial m}\left[\nu_2\phi_3 L_{22}\frac{\partial\mu_2}{\partial m}\right] \qquad [22]$$

The main factor determining the type of demixing process is the local concentration in the film. Using eqns [21] and [22] it is possible to calculate these concentrations ($\phi_1$, $\phi_2$, $\phi_3$) as a function of time. Thus at any time and any place in a cast film the demixing process occurring can be calculated; in fact the concentrations are calculated as a function of place and elapsed time and the type of demixing process is deduced from these values. However, one should note that a number of assumptions and simplifications are involved in this model. Thus heat effects, occurrence of crystallization and relative molecular mass distributions are not taken into account. Nevertheless, it will be shown in the next section that the model allows the type of demixing to be established on a qualitative basis and is therefore useful as a first estimate. Furthermore, it allows an understanding of the fundamentals of membrane formation by phase inversion.

### Mechanism of Membrane Formation

It is shown in this section that two types of demixing process resulting in two different types of membrane morphology can be distinguished:

- instantaneous liquid–liquid demixing, where the membrane is formed immediately;
- delayed onset of liquid–liquid demixing, where the membrane takes some time to form.

The occurrence of these two distinctly different mechanisms of membrane formation can be demonstrated in a number of ways: by calculating the concentration profiles; by light transmission measurements; and visually.

The best physical explanation is given by a calculation of the concentration profiles. To calculate the

concentration profiles in the polymer film during the delayed demixed type of phase inversion process, some assumptions and considerations must be made:

- diffusion in the polymer solution;
- diffusion in the coagulation bath – no convection occurs in the coagulation bath;
- thermodynamic equilibrium is established at the film–bath interface:
  $\mu_i$ (film) = $\mu_i$ (bath) $\quad i = 1, 2, 3$;
- volume fluxes at the film–bath interface are equal, i.e.
  $J_i$ (film) = $J_i$ (bath) $\quad i = 1, 2$.

In addition, the thermodynamic binary interaction parameters (the $\chi$ parameters or the concentration-dependent $g$ parameters) that appear in the expressions for the chemical potentials must be determined experimentally.

- $g_{12}$, from calorimetric measurements yielding values of the excess free energy of mixing, from literature compilations of $G^E$ and activity coefficients, from vapour–liquid equilibria and from Van Laar, Wilson, or Margules equations or from UNIFAC;
- $g_{13}$, from equilibrium swelling experiments or from inverse gas chromatography,
- $g_{23}$, from membrane osmometry or vapour pressure osmometry.

Two types of demixing process will now be distinguished that lead to different types of membrane structure. These two different types of demixing process may be characterized by the instant when liquid–liquid demixing sets in. **Figure 19** shows the composition path of a polymer film schematically at the very instant of immersion in a nonsolvent bath (at $t < 1$ s). The composition path gives the concentration at any point in the film at a particular time. For any other time, another compositional path will exist.

Because diffusion processes start at the film–bath interface, the change in composition is first noticed in the upper part of the film. This change can also be observed from the composition paths given in Figure 19. Point $t$ gives the composition at the top of the film while point $b$ gives the bottom composition. Point $t$ is determined by the equilibrium relationship at the film–bath interface $\mu_i$ (film) = $\mu_i$ (bath). The composition at the bottom is still the initial concentration in both examples. In Figure 19A places in the film beneath the top layer $t$ have crossed the binodal curve, indicating that liquid–liquid demixing starts immediately after immersion. In contrast, Figure 19B indicates that all compositions directly beneath the top layer still lie in the one-phase region and are still miscible. This means that no demixing occurs immediately after immersion. After a longer time interval, compositions beneath the top layer will cross the binodal curve and liquid–liquid demixing will start in this case also. Thus two distinctly different demixing processes can be distinguished and the resulting membrane morphologies are also completely different.

When liquid–liquid demixing occurs instantaneously, membranes with a relatively porous top layer are obtained. This demixing mechanism results in the formation of a porous membrane (microfiltration/ultrafiltration type). However, when liquid–liquid demixing sets in after a finite period of time, membranes with a relatively dense top layer are obtained. This demixing process results in the formation of dense membranes used for gas separation/pervaporation. In both cases the thickness of the top

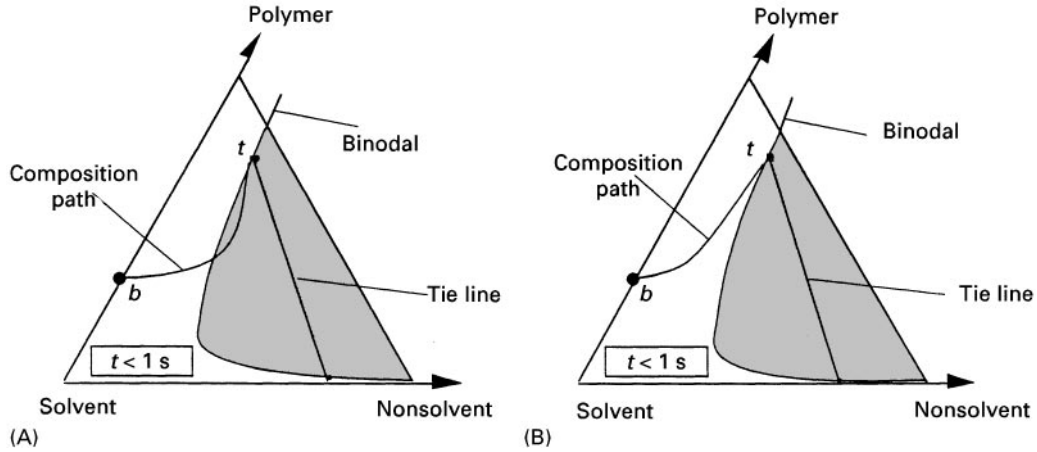


**Figure 19** Schematic composition path of the cast film immediately after immersion; $t$ is the top of the film and $b$ is the bottom. Part (A) shows instantaneous liquid–liquid demixing whereas (B) shows the mechanism for the delayed onset of liquid–liquid demixing.

**Table 4** Polymers that are frequently used as phase inversion membranes

| *Polymer* | *Process* |
|---|---|
| Cellulose acetate | MF, UF, NF, RO, GS |
| Nitrocellulose | MF |
| Polysulfone | MF, UF |
| Polyethersulfone | MF, UF |
| Polyacrylonitrile | MF, UF |
| Polyvinylidenefluoride | MF, UF |
| Polyimide | UF, GS |
| Aliphatic polyamide | MF, UF |
| Aromatic polyamide | NF, RO |
| Polyphenylene oxide | GS |

MF, microfiltration; UF, ultrafiltration; NF, nanofiltration; RO, reverse osmosis; GS, gas separation.

layer is dependent on a variety of membrane formation parameters (i.e. polymer concentration, coagulation procedure, additives, etc.).

### Polymers for Phase Inversion Membranes

The preparation of phase inversion membranes has only been described briefly. It may be evident that many polymers can be applied as long as they are soluble in a suitable organic solvent. This is the only limitation. Nevertheless, owing to their mechanical, thermal and chemical properties some polymers are more frequently applied. Two of these so-called 'engineering polymers', polysulfone and polyethersulfone, are used as micro- and ultrafiltration membranes or as support material in composite membranes for nanofiltration, reverse osmosis and gas separation. These two polymers have very good film-forming properties and are soluble in a range of solvents. Beside these two polymers a wide variety of other polymers are applied; these are listed in **Table 4**.

## Future Developments

Phase inversion will remain the most important technique for the preparation of polymeric membranes for microfiltration and ultrafiltration membranes and for use as support membranes in composite membranes for nanofiltration, reverse osmosis, gas separation, vapour permeation and pervaporation.

*See also:* **III/Membrane Preparation:** Hollow Fibre Membranes; Interfacial Composite Membranes

## Further Reading

Arnauts J and Berghmans H (1987) Atactic gels of atactic polystyrene. *Polymer Communications* 28: 66–68.

Altena FW and Smolders CA (1982) Calculation of liquid–liquid phase separation in a ternary system of a polymer in a mixture of a solvent and a nonsolvent. *Macromolecules* 15: 1491–1497.

Altena FW, Smid J, Van den Berg JWA, Wijmans JG and Smolders CA (1985) Diffusion from solvent from a cast CA solution. *Polymer* 26: 1531.

Boom RM, Wienk IM, Boomgaard van den T and Smolders CA (1992) Microstructures in phase inversion membranes. Part 2, the role of the polymer additive. *Journal of Membrane Science* 73: 277–292.

Boom RM, Boomgaard van den T and Smolders CA (1994) Mass transfer and thermodynamics during immersion precipitation for a two-polymer system: evaluation with the systems PES-PVP-NMP-water. *Journal of Membrane Science* 90: 231–249.

Bulte AMW, Folkers B, Mulder MHV and Smolders CA (1993) Membranes of semi-crystalline aliphatic polyamide Nylon 4-6. Formation by diffusion induced phase separation. *Journal of Applied Polymer Science* 50: 13–26.

Caneba GT and Soong DS (1985) Polymer membrane formation through the thermal inversion process. 1. Experimental study of membrane formation. *Macromolecules* 18: 2538–2545.

Caneba GT and Soong DS (1985) Polymer membrane formation through the thermal inversion process. 2. Mathematical modeling of membrane structure formation. *Macromolecules* 18: 2545–2555.

Cheng L-P, Soh YS, Dwan A-H and Gryte CC (1994) An improved model for mass transfer during the formation of polymer membranes by the immersion precipitation process. *Journal of Polymer Science Part B, Polymer Physics* 32: 1413–1425.

Cohen C, Tanny GB and Prager EM (1979) Diffusion-controlled formation of porous structures in ternary polymer systems, *Journal of Polymer Science, Polymer Physics Edition* 17: 477–489.

Eykamp W (1995) Microfiltration and ultrafiltration. In: Noble RD and Stein A (eds) *Membrane Separation Technology, Principles and Applications*, pp. 1–25. Amsterdam: Elsevier.

Ferry D (1936) Ultrafilter membranes and ultrafiltration. *Chemical Reviews* 18: 373–455.

Flory PJ (1953) *Principles of Polymer Chemistry*. Ithaca, NY: Cornell University Press.

Gaides GE and McHugh AJ (1989) Gelation in an amorphous polymer: a discussion of its relation to membrane formation. *Polymer* 30: 2118–2123.

Guillotin M, Lemoyne C, Noel C and Monnerie L (1977) Physicochemical processes occurring during the formation of cellulose diacetate membranes. Research of criteria for optimizing membrane performance. IV. cellulose diacetate-acetone-organic additive casting solutions. *Desalination* 21: 165–170.

Kamide K and Matsuda S (1984) Phase equilibria of quasi ternary systems consisting of multi-component polymers in a binary solvent mixture. II Role of initial concentration and relative amount of polymers. *Polymer Journal* 7: 515–530.

Koenhen DM, Mulder MHV and Smolders CA (1977) Phase separation phenomena during the formation of asymmetric membranes. *Journal of Applied Polymer Science* 21: 199–215.

Lloyd DR and Kinzer KE (1991) Microporous membrane formation via thermally induced phase separation. II Liquid–liquid phase separation. *Journal of Membrane Science* 64: 1–11.

McHugh AJ and Yilmaz L (1985) The diffusion equation for polymer membrane formation in ternary systems. *Journal of Polymer Science*, *Polymer Physics Edition* 23: 1271–1274.

McHugh AJ and Tsay CS (1992) Dynamics of the phase inversion process. *Journal of Applied Polymer Science* 46: 2011–2021.

Mulder MHV, Oude Hendrikman J, Wijmans JG and Smolder CA (1985) A rationale for the preparation of asymmetric pervaporation membranes. *Journal of Applied Polymer Science* 30: 2805–2830.

Mulder MHV, Franken ACM and Smolders CA (1985) Preferential sorption versus preferential permeation. *Journal of Membrane Science* 22: 155–173.

Mulder MHA (1996) *Basic Principles of Membrane Technology*. Dordrecht: Kluwer.

Radovanovic P, Thiel SW and Hwang S-T (1992) Formation of asymmetric polysulfone membranes by immersion precipitation. Part II. The effects of casting solution and gelation bath compositions on membrane structure and skin formation. *Journal of Membrane Science* 65: 231.

Radovanovic P, Thiel SW and Hwang S-T (1992) Formation of asymmetric polysulfone membranes by immersion precipitation. Part I. Modelling of mass transport during gelation. *Journal of Membrane Science* 65: 213–229.

Reuvers AJ, Altena FW and Smolders CA (1986) Demixing and gelation behaviour of ternary cellulose acetate solutions studied by differential scanning calorimetry. *Journal of Polymer Science*, *Polymer Physics Edition* 24: 793–804.

Reuvers AJ, Berg van den JWA and Smolders CA (1987) Formation of membranes by means of immersion precipitation. Part I. A model to describe mass transfer during immersion precipitation. *Journal of Membrane Science* 34: 45–65.

Reuvers AJ and Smolders CA (1987) Formation of membranes by means of immersion precipitation. Part II. The mechanism of membranes prepared from the system cellulose acetate–acetone–water. *Journal of Membrane Science* 34: 67–86.

Strathmann H, Koch K, Amar P and Baker RW (1975) The formation mechanism of asymmetric membranes. *Desalination* 16: 179–203.

Tan HM, Moet A, Hiltner A and Baer E (1983) Thermoreversible gelation of atactic polystyrene solutions. *Macromolecules* 16: 28–34.

Tsai FJ and Torkelson JM (1990) Roles of phase separation mechanism and coarsening in the formation of PMMA asymmetric membranes. *Macromolecules* 23: 775–784.

Tsay CS and McHugh AJ (1990) Mass transfer modelling of asymmetric membrane formation by phase inversion. *Journal of Polymer Science* 28: 1327–1365.

Tsay CS and McHugh AJ (1991) Mass transfer dynamics of the evaporation step in membrane formation by phase inversion. *Journal of Membrane Science* 64: 81–92.

Tsay CS and McHugh AJ (1991) The combined effects of evaporation and quench steps on asymmetric membrane formation by phase inversion. *Journal of Polymer Science Part B*, *Polymer Physics* 29: 1261–1270.

Vadalia HC, Lee HK, Myerson HS and Levon K (1994) Thermally induced phase separation in ternary crystallizable polymer solutions. *Journal of Membrane Science* 89: 37–50.

Wisniak J and Tamir A (1978) *Mixing and Excess Thermodynamic Properties*. Amsterdam: Elsevier.

Wijmans JG, Kant J, Mulder MHV and Smolders CA (1985) Phase separation phenomena in solutions of polysulfone in mixtures of a solvent and a nonsolvent: relationship with membrane formation. *Polymer* 26: 1539–1545.

Wijmans JG, Rutten HJJ and Smolders CA (1985) Phase separation phenomena in solutions of PPO in mixtures of trichloroethylene, octanol and methanol: relation to membrane formation. *Journal of Polymer Science*, *Polymer Physics* 23: 1941–1955.

Yilmaz L and McHugh AJ (1986) Analysis of solvent–nonsolvent–polymer phase diagrams and their relevance to membrane formation modelling. *Journal of Applied Polymer Science* 31: 997–1018.

Yilmaz L and McHugh AJ (1986) Modelling of asymmetric membrane formation. I. Critique of evaporation models and development of diffusion equation formalism for the quench period. *Journal of Membrane Science* 28: 287–310.

Zeman L and Tkacik G (1988) Thermodynamic analysis of a membrane forming system water–*N*-methyl-2-pyrrolidone/polyethersulfone. *Journal of Membrane Science* 36: 119–140.

# METABOLITES

*See* **III / DRUGS AND METABOLITES: Liquid Chromatography-Mass Spectrometry; Liquid Chromatography-Nuclear Magnetic Resonance-Mass Spectrometry**